Proceedings of Meetings on Acoustics

Volume 2, 2008 http://asa.aip.org

154th Meeting
Acoustical Society of America
New Orleans, Louisiana
27 November - 1 December 2007
Session 2aPP: Psychological and Physiological Acoustics

2aPP1. Probing the temporal resolution and bandwidth of human hearing

Milind N. Kunchur*

***Corresponding author's address: Physics and Astronomy, University of South Carolina, Columbia, S.C. 29208, kunchur@sc.edu**

Experiments were conducted to assess the human discriminability of temporal convolution. The experiments employed either lowpass filtering or delays due to spatial misalignment. By using special ultrahigh-fidelity equipment, both experiments demonstrated discernment at a ~ 5 microsecond timescale, which is much shorter than found previously. While the signal manipulations affect both the spectrum and temporal definition of the signal, the spectral changes fall below the known just noticeable differences. The discrimination may therefore involve mechanisms additional to the auditory system's ability to distinguish spectral amplitude differences. Furthermore the present work shows that typical instrumentation used in psychoacoustic research may, for some purposes, have insufficient temporal speed and bandwidth. Also this work proves that that digital sampling rates used in consumer audio are insufficient for fully preserving transparency.

Published by the Acoustical Society of America through the American Institute of Physics

For related papers and answers to FAQs please see: http://www.physics.sc.edu/kunchur/Acoustics-papers.htm

Received 19 Jun 2008; published 22 Sep 2008

INTRODUCTION

In linear systems, the characteristic response time τ is inversely proportional to the upper frequency limit f_C, and typically $\tau \sim 1/\omega_C = 1/2\pi f_C$. Complexities of auditory neurophysiology can negate this simple reciprocal relationship allowing for the possibility of a threshold t well below the nominally expected $[2\pi 18\text{kHz}]^{-1}$=9 μs. While anecdotal evidence in high-end audio suggests this to be true (van Maanen, 1993; Woszczyk, 2003; Stuart, 2004), formal psychoacoustic experiments (for example, Plomp, 1964; Ronken, 1970; Leshowitz, 1971; Henning, 1974; Nordmark, 1976; Penner, 1977; Henning and Gaskell, 1981; Eddins et al., 1992; Yost et al., 1996; Patterson and Datta, 1996; Krumbholz et al., 2003) have not confirmed this. The present work revisited this issue using improved gating methods and special ultrahigh-fidelity equipment. In order to overcome some of the deficiencies in traditional instrumentation, the following changes were made: (1) Digital synthesis was replaced by an analog signal source (which was a thousand times faster than CD quality digital audio). (2) Typical transducers (e.g., TDH-39) were replaced with high-end headphones (Grado RS1) and fast ribbon tweeters (Aurum Cantus G2Si). (3) Custom amplifiers were built with specs (τ_{rise} < 0.1 μs, R_{out} < 50 μW, noise/distortions ~ 0) far superior to typical commercial units. And (4) Traditional onset/offset ramps, which insert a silent gap between stimuli, were replaced by perfectly continuous transition and three new approaches to gating were developed for this purpose. The end result is that this work demonstrated a temporal discrimination of ~5 μs (i.e., an ultrasonic-range cutoff of f_C ~ 32 kHz).

EXPERIMENTS

Experiment 1

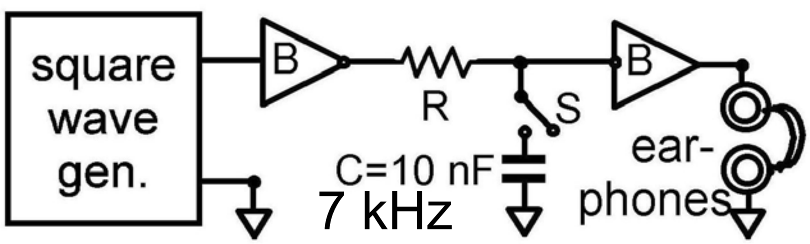

Figure 1: Functional diagram of circuitry used in experiment 1.

In this experiment, listeners were required to distinguish low-pass filtered (switch S closed) and unfiltered (S open) 7 kHz square-wave tones. The time constant t = RC (please see Fig. 1) was varied to determine the threshold for discrimination. Careful design and construction (point-to-point wiring, close-return geometry, ultrahigh quality components, etc.) ensured a perfectly continuous moving spectrum and absence of audible transients. The following oscillogram (Fig. 2) show how the signal continues where it left off when the filter is switched out with no transient or other anomaly.

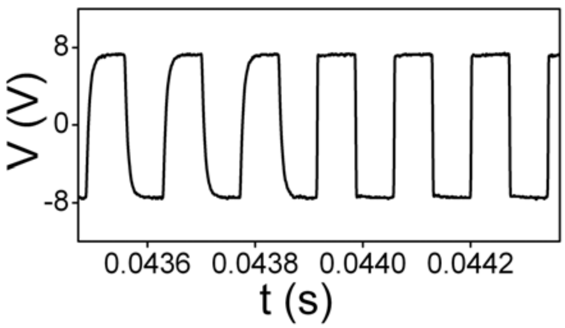

Figure 2: Oscilloscope trace showing a clean transition between filtered to unfiltered signals.

Gating integrity was confirmed by a blind test that checked whether listeners can hear a transient while an ultrasonic 22 kHz signal is passed through the circuit. The statistics in Table 1 (below) show an absence of audibility.

% correct	HR	FAR	d'	c	χ2
46%	0.06	0.10	-0.32	1.26	0.64

Table 1: Results of 100 blind trials (20 trials on each of 5 subjects) in which a 22 kHz square wave signal was switched from filtered to unfiltered. The results show an absence of audibility of the gating event.

The figure below shows the acoustic waveform of the output of the headphone measured using a flat-plate coupler and an ACO Pacific microphone.

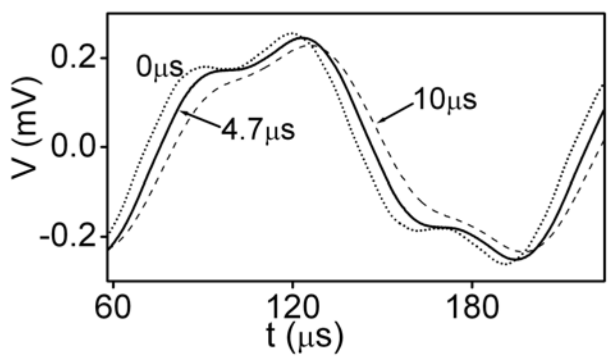

Figure 3: Waveforms of the acoustic output of the headphones for τ = 0, 4.7, and 10 μs.

The figure of the unsynchronized spectrum below (Fig. 4) prove an absence of anharmonic distortion and hence an exact periodicity of the acoustic signal.

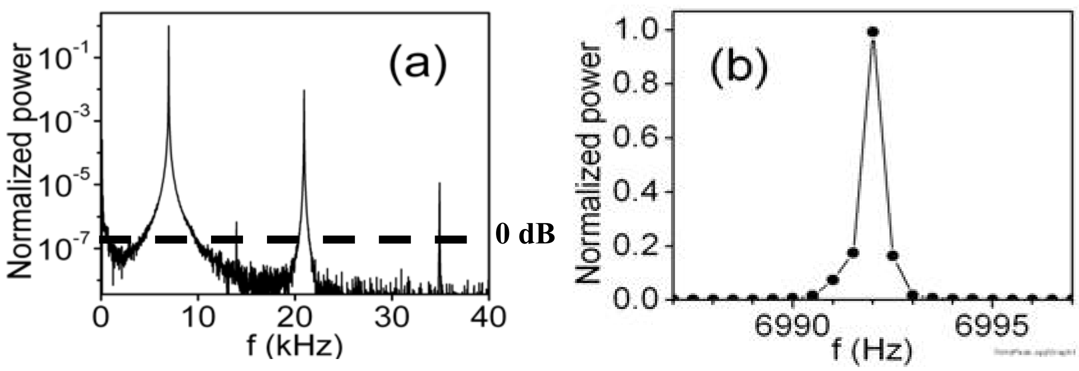

Figure 4: Power spectrum of the unaveraged acoustic output from the headphone normalized to the power coefficient of the fundamental peak.

In view of the exact periodicity, the signal can then be represented by a Fourier series of the type:

$$V(t) = \Sigma C_n \cos(2\pi f_n t + \theta_n) \text{ where } f_n = 7000n \text{ Hz} \tag{1}$$

The table below gives the coefficients of this Fourier representation of the acoustic waveform. Note that only the 7 kHz component is audible since the higher harmonics have levels that are subliminal as per ISO (MAF) standard: ISO 389-7 (1996). Note that the noise floor of ~ 0.0003 ~ 1/4096 equals the quantization error of the (12 bit) digital oscilloscope.

τ	f_1=7 kHz		f_2=14 kHz		f_3=21 kHz		f_5=35 kHz	
(μs)	C_1	θ_1	C_2	θ_2	C_3	θ_3	C_5	θ_5
0	1.0000	0.00	0.0003	2.30	0.2167	2.40	0.0183	1.89
3.9	0.9825	0.00	0.0004	2.36	0.1921	2.36	0.0139	1.73
4.7	0.9791	0.00	0.0004	2.23	0.1843	2.34	0.0128	1.64
5.6	0.9715	0.00	0.0004	2.27	0.1753	2.31	0.0116	1.52
6.8	0.9580	0.00	0.0004	2.03	0.1632	2.25	0.0102	1.35
7.7	0.9503	0.00	0.0004	2.12	0.1583	2.21	0.0094	1.18
10	0.9147	0.00	0.0004	2.03	0.1340	2.07	0.0076	0.84
30	0.6070	0.00	0.0003	1.48	0.0564	0.96	0.0030	4.81

τ	f_7=49 kHz		f_9=63 kHz		f_{11}=77 kHz		f_{13}=91 kHz	
(μs)	C_7	θ_7	C_9	θ_9	C_{11}	θ_{11}	C_{13}	θ_{13}
0	0.0040	5.26	0.0027	3.48	0.0028	5.68	0.0031	2.90
3.9	0.0026	4.97	0.0015	2.93	0.0024	4.90	0.0008	1.84
4.7	0.0022	4.83	0.0014	2.72	0.0020	4.58	0.0007	1.46
5.6	0.0020	4.64	0.0012	2.48	0.0017	4.22	0.0006	1.04
6.8	0.0016	4.39	0.0010	2.15	0.0014	3.73	0.0005	0.52
7.7	0.0013	4.05	0.0009	1.90	0.0012	3.31	0.0005	0.05
10	0.0009	3.50	0.0006	1.31	0.0009	2.34	0.0003	5.15
30	0.0004	0.06	0.0002	3.33	0.0003	3.14	0.0001	5.31

Table 2: Harmonic contents of acoustic signals. $C_n(\tau)$'s are expressed as a fraction of $C_1(0)$. $\theta_n(\tau)$'s are expressed relative to $\theta_1(\tau)$.

Experiment 2

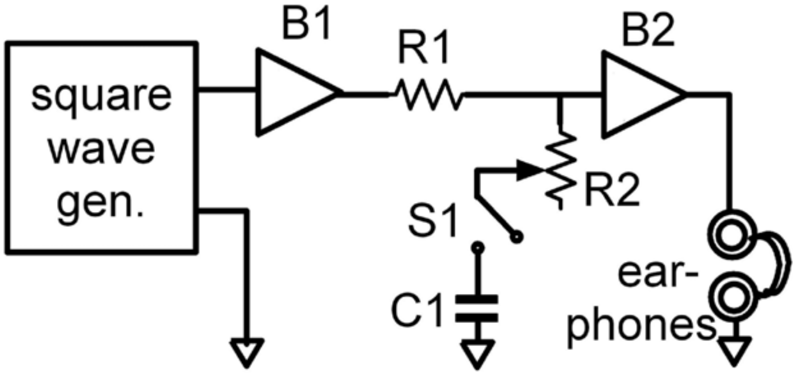

Figure 5: Functional diagram of circuitry used in experiment 2.

The setup for this experiment is almost identical to Expt. 1 except a potentiometer R2 (variable resistor) is placed in series with the switch S1. The listeners' task was to turn the potentiometer from one side to the other and listen for a difference and thus judge whether the switch S1 was closed or not. Here the transition from filtered to unfiltered took place gradually over ~3 s (21,000 cycles). The potentiometer was of high quality (Noble) to ensure noise-free performance. The purpose of this experiment was to further verify that the method of gating exerted no influence and also to add statistics to the $\tau = 5.6$ µs measurement.

Experiment 3

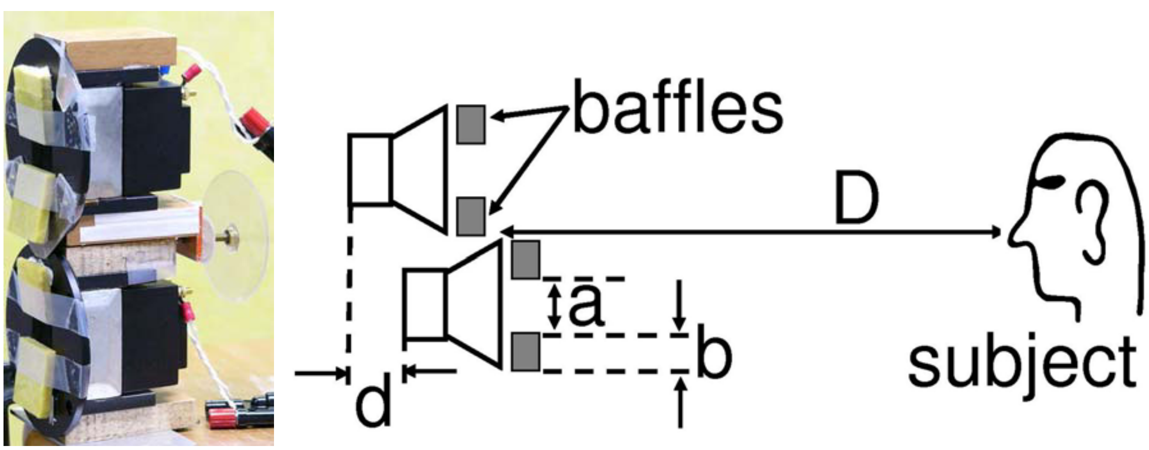

Figure 6: Functional diagram of apparatus used in experiment 3.

In this third experiment, the temporal change is effected by spatial (acoustic) displacement rather than electronically. Here, a=1.5cm, b=4.3cm, D=4.3m, *d*=2-10mm. Electronics similar to the previous experiments provided a 7 kHz square-wave signal to the two stacked ribbon tweeters, whose apertures were narrowed by baffles to reduce intrinsic temporal spreads. Rails and a micrometer screw provided controllable amounts of misalignments *d*. From the barely discernable *d* we get the threshold t = *d/vsound*.

Once again absence of anharmonic distortion and other artifacts was ascertained as before. Figures of the spectrum (left) and waveforms (right) are shown below:

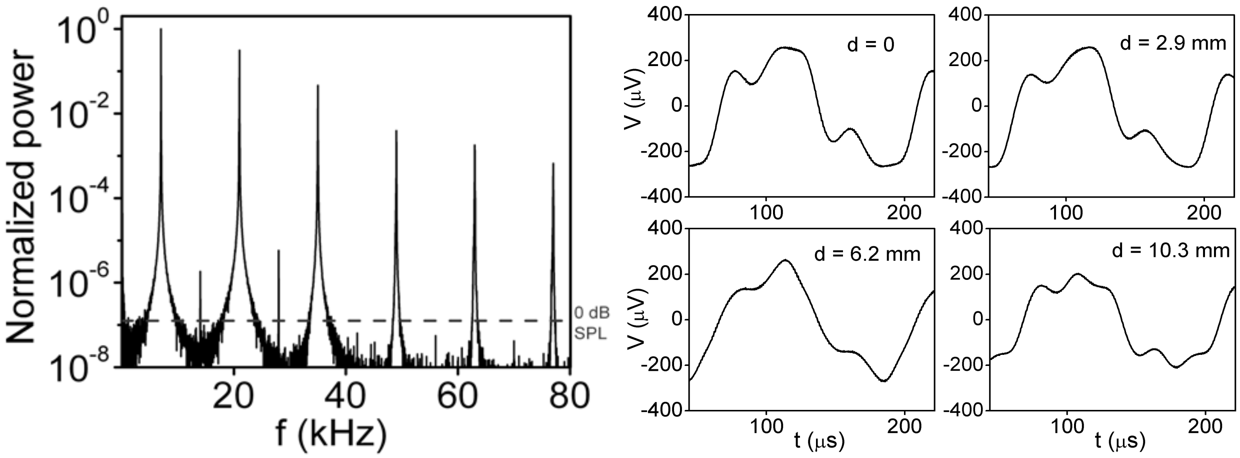

Figure 7: Spectrum and waveforms of acoustic signals in experiment 3.

The room environment was made as anechoic as possible but reflected energy, if any, folds into the superposition anyway; the superposition for the aligned position being given by

$$A\cos(2\pi f[t+l'/c])+A\cos(2\pi ft) = \sum_n A_n\cos(2\pi f[t+(D_n+l_n)/c])+\sum_n A_n\cos(2\pi f[t+D_n]) \tag{2}$$

and the superposition for the misaligned position being given by

$$A\cos(2\pi f[t+\{l'+d'\}/c])+A\cos(2\pi ft) = \sum_n A_n\cos(2\pi f[t+\{d_n+D_n+l_n\}/c])+\sum_n A_n\cos(2\pi f[t+D_n]) \tag{3}$$

The Fourier representation of acoustic waveform at listener position is given by

$$V(t) = \Sigma C_n\cos(2\pi f_n t+\theta_n) \text{ where } f_n = 7000n \text{ Hz} \tag{4}$$

with the values of the Fourier coefficients as given in Table 3 (below). Once again only the 7 kHz component is at an audible level.

d	f_1=7 kHz		f_2=14 kHz		f_3=21 kHz		f_5=35 kHz	
(mm)	C_1	θ_1	C_2	θ_2	C_3	θ_3	C_5	θ_5
0	1.000	0.00	0.006	-3.81	0.332	-1.29	0.145	-0.84
2.9	0.973	0.00	0.006	-4.09	0.329	-1.54	0.104	-1.66
6.2	0.933	0.00	0.005	-4.49	0.217	-1.50	0.038	-5.35
10.3	0.816	0.00	0.004	-5.48	0.156	-0.67	0.131	-0.11

d	f_7=49 kHz		f_9=63 kHz		f_{11}=77 kHz		Attenuation	
(mm)	C_7	θ_7	C_9	θ_9	C_{11}	θ_{11}	rms	C_1
0	0.018	-1.94	0.007	-3.02	0.002	-3.79	0	0
2.9	0.012	-3.09	0.003	-4.50	0.001	-0.10	0.26	0.24
6.2	0.013	-0.90	0.008	-2.62	0.002	-4.13	0.90	0.60
10.3	0.007	-1.98	0.005	-1.16	0.002	-2.98	2.03	1.76

Table 3: Harmonic contents of acoustic signals. $C_n(\tau)$'s are expressed as a fraction of $C_1(0)$. $\theta_n(\tau)$'s are expressed relative to $\theta_1(\tau)$.

RESULTS

Results for Experiment 1

Group 1 subjects (5) were given 10 trials each at all τ values; group 2 subjects (2) were given 25 trials at τ = 5.6 μs. The Table 4 (below) shows the results. Here f_{max} is the upper audibility limit for pure tones at 69 dB SPL.

Subject	f_{max} (kHz)	30 μs	10 μs	7.7 μs	6.8 μs	5.6 μs	4.7 μs	3.9 μs
S1	17.8	10	10	10	10	10	10	5
S2	16.6	10	10	10	10	10	10	5
S3	17.7	10	10	10	10	10	8	8
S4	14.8	10	10	10	10	10	8	5
S5	9.4	10	10	10	10	10	7	4

Table 4: Results of blind trials for experiment 1. The rows correspond to different subjects. The first column gives the high-frequency threshold for pure tones at a level of 69 dB SPL. Other entries indicate number of correct judgements (out of 10).

A second group of (2) subjects was tested at just τ = 5.6 μs with the results shown in the table below.

Subject	f_{max} (kHz)	5.6 μs
S6	15.0	25/25
S7	17.0	25/25

Table 5: Additional results of blind trials for experiment 1 (2 new subjects tested at just τ=5.6 μs).

Results for Experiment 2

In this experiment employing low-pass filtering with gradual transition the results on a third group of (3) subjects is shown in the table below. The cumulative statistics for Expts. 1 and 2 (groups 1, 2 & 3) at τ = 5.6 μs are: 10 subjects, 220 trials, χ^2 = 220, and 100% correct judgements. The results of Expts. 1 and 2 are discussed in Kunchur (2008).

Subject	f_{max} (kHz)	**5.6** μs
S8	14.6	40/40
S9	16.1	40/40
S10	14.4	40/40

Table 6: Results of blind trials for experiment 2.

Results for Experiment 3

Results for the speaker-displacement experiment are shown below. The threshold delay, obtained by dividing the threshold displacement by the speed of sound, was found to be τ ~ 6 μs. The results of Expt. 3 are discussed in Kunchur (2007).

Subject	**10.3mm** 30 μs	**6.2mm** 18μs	**3.9mm** 11 μs	**2.9mm** 8.4 μs	**2.3mm** 6.7 μs	**2.0mm** 5.8 μs
S11	10	10	10	10	9	10
S12	10	10	10	10	8	4
S13	10	10	10	10	10	4
S14	10	10	10	10	9	4
S15	10	10	10	10	5	4

Table 7: Results of blind trials for experiment 3. The rows correspond to different subjects. Entries correspond to scores out of 10 blinds trials for each subject for each displacement.

DISCUSSION

Three experiments, using different methodologies to introduce temporal smearing, found thresholds in the τ ~ 5—6 μs range. This threshold is shorter than the nominal $[2\pi 18\text{kHz}]^{-1}$=9 μs. What can be the basis of this discrimination? The stimuli are periodic and have identical frequencies in their spectra. Their differences are summarized by the levels and phases of mainly the 7 kHz and 21 kHz components. The level differences are given by the attenuation formulas:

$$\Delta L_p = -10\log[1+(2\pi f\tau)^2] \text{ (RC low-pass filter).} \tag{5}$$

$$\Delta L_p = -10\log\left[\frac{\cos^2\{\pi f(d+l')/c\}}{\cos^2\{\pi f l'/c\}}\right] \text{ (speaker displacement).} \tag{6}$$

These calculated values agree well with measured attenuations (taking the C_n's from the Fourier coefficient tables):

$$\Delta L_p = 20\log[C_n] \text{ (measured attenuation).} \tag{7}$$

These level changes by themselves ought to be subliminal based on the level JND measurements of Jesteadt, Wier, and Green, (1977). Attenuations in the present experiments at threshold are about 0.2 dB (4% change in power), whereas the JND is 0.7 dB (15% change in power). Even the 3-standard-error lower limit of the JND is 0.5 dB (11 % change in power).

On the other hand, while level changes may be subliminal, phase shifts for the ultrasonic components are significant; 21 kHz shifts by 32°. How could this become audible? Through nonlinear mixing. Nonlinearities can generate a 14 kHz component through two routes: (1) by a doubling of the 7 kHz and (2) as a difference between 7 kHz and 21 kHz. These two 14 kHz contributions are phase locked to their originating 7 kHz and 21 kHz components. Furthermore, they are coherent and can interfere. Converting from the initial acoustic signal to an internal representation, we can now trace the successive alterations in the signal to find how the nonlinear 14 kHz product might change with temporal manipulations in the present experiments.

$$\begin{array}{l}\underline{\text{Initial acoustic signals (see earlier Fourier table):}}\\ K''[0.98\cos(2\pi 7000t)+0.18\cos(2\pi 21000t+\phi''_A)]\\ K''[\cos(2\pi 7000t)+0.22\cos(2\pi 21000t+\phi''_B)]\end{array} \tag{8}$$

$$\begin{array}{l}\underline{\text{External+middle ear filtering (Glasberg and Moore, 1990):}}\\ K'[0.98\cos(2\pi 7000t)+0.15\cos(2\pi 21000t+\phi'_A)]\\ K'[\cos(2\pi 7000t)+0.19\cos(2\pi 21000t+\phi'_B)]\end{array} \tag{9}$$

The result of nonlinear mixing of the above results in:

$$\begin{array}{l}\text{For a nonlinear response represented by } y\propto x+bx^2\\ \text{an input } x\propto \cos\omega_0 t+a\cos(3\omega_0 t+\theta)\\ \text{gives rise to } y\propto\cos\omega_0 t+\frac{b}{2}\cos(2\omega_0 t)+ab\cos(2\omega_0 t+\theta)\end{array} \tag{10}$$

the three terms on the R.H.S. corresponding to the linear, quadratic, and difference terms respectively. The quadratic and difference terms (both 14 kHz) can interfere through the phase shift θ, which is locked to the 21 kHz phase. For $\tau = RC = 4.7$ μs, $\theta = 20°$. From this, one can calculate the level change in the 14 kHz power:

$$\Delta L_p(14\text{ kHz})=10\log\left(\frac{[0.5+0.19\sin(\Delta\phi/2)]^2}{[0.5\times 0.98^2+0.15\times 0.98\sin(-\Delta\phi/2)]^2}\right)=1.4\text{dB} \tag{11}$$

This level change is eight times larger than the subliminal 0.18 dB level change of the 7 kHz fundamental component, although the upper audibility limit of the listener needs to be higher than 14 kHz for the level of the proposed nonlinear mechanism to work. In the reference Kunchur (2007), an estimate is obtained for the temporal resolution of transient signals (the present experiments use periodic and not transient signals) based on the synchronous convergence of cross frequency auditory-nerve (AN) signals. Interestingly this estimate of τ ~ 2—16 μs agrees with the τ = 5—6 μs range measured here.

CONCLUSION

This research found audibility of temporal alterations on a ~5 μs time scale. On the one hand this confirms anecdotal claims in high-end audio that performance in the ultrasonic range is required to maintain fidelity in the audible range. On the other hand it also points to the need for higher bandwidths in apparatus used in psychoacoustic research for certain types of experiments, so that the thresholds measured are not affected by the limitations of the equipment.

While both amplitudes and phases are altered by the temporal manipulation, the effect of phase appears to be more significant than the effect of level change (which in fact appears to be subliminal) by the time the signal reaches its internal representation. Thus the source of the discrimination may be related to the change in the waveform shape rather than just its power.

An improvement in the present experiments over past experiments in the psychoacoustic literature is the use of specially designed ultrahigh fidelity equipment throughout the signal chain. An enormous time (of the order of two years) and effort were spent to develop the instrumentation and the methods for checking for artifacts. For example, for just the Fourier spectrum shown in Fig. 4, it took a few months to develop the instrumentation setup and to write the C code (FFT was not used). To measure one such spectrum takes over a week. Notice that the noise level is below 0 dB SPL. Without performing such tests, it will not be known exactly what frequency components are present and what their roles are in the discernment. To simply trust the instructions given to a signal synthesizer and expect that, that is what actually comes out is risky.

Another key difference in the present work is the use of analog signal sources and analog signal processing (using an RC filter or a mechanical spatial displacement). Typical digital signal sources and digital processing cannot achieve exactly the same results and are likely to produce artifacts that may mask the changes being discerned. It is very difficult to produce an exactly periodic waveform (of any shape) digitally. Jitter (which is usually a serious problem) introduces cycle-to-cycle variations in the period. The ear is extremely sensitive to this jitter. As found by Pollack (1969 and 1971) a variation of as little as 100 ns (a variation of 0.1% in the period) can be discerned. The analog square-wave signal source used in the present work has a jitter of 68 ns (<0.05% of the period). One should carefully check the actual acoustic spectrum, as done in Fig. 4, to make ascertain the actual composition of the signal. The typical commercial spectrum analyzer might not be able to perform this task with the required combination step size, record length, vertical resolution, and dynamic range. It may be better to take long digital records (the frequency steps in the spectrum will be inversely proportional to the record length), compute their spectrum, store it, and repeat this process. The separate spectra can then be averaged together to reduce noise until enough have been accumulated and averaged to obtain the required signal-to-noise ratio.

Another problem that arises with digital synthesis is that it can produce exactly periodic signals for only a small subset of frequencies (even if jitter is absent). This is because of the quantization. While elaborate interpolation techniques, oversampling, and upsampling may mitigate this problem, it is always present. Let's take the simplest task of producing a 1 volt amplitude periodic square waveform such as 7 kHz (used in the present work) using a sampling rate of 192 kHz. It cannot be done! The signal will need to be at +1 V for 1/14,000 s then go to -1V for 1/14,000 s and repeat this indefinitely. However the digital synthesizer can only be +1V or -1V (assuming that its vertical steps allow this) for durations that are integer multiples of 1/192,000 s (i.e., n times 5.208 μs). However 1/14,000 s is not exactly divisible by 5.208 μs (in fact 192,000/14,000 = 13.71). This means that all cycles cannot be of the same duration and periodicity will be lost (extraneous frequencies will join the spectrum). As an illustration of this effect, Fig. 8 shows the digital representation (screen snapshot of the Sony Sound Forge software window) of 1850 Hz at a sampling rate of 8000 Hz. Notice how some periods are longer than others. At higher sampling rates this "catch-up period" will occur less frequently but will always be there except when the sampling period and exactly divides the signal half period. Note that this problem is mathematical and occurs regardless of, and in addition to, instrumental distortions and problems.

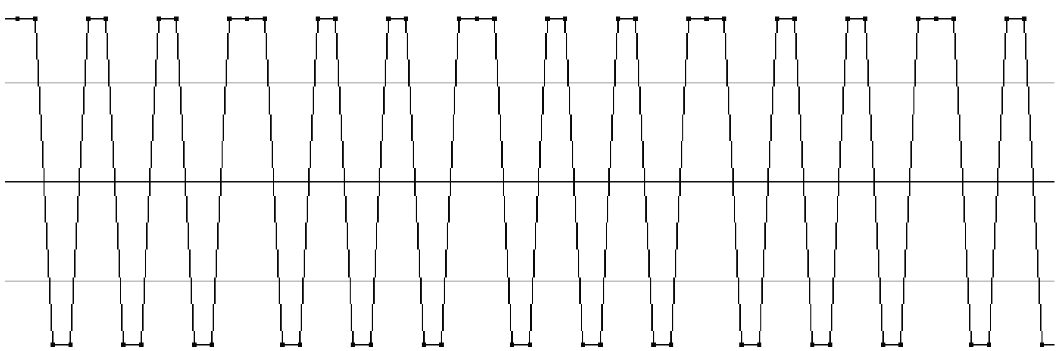

Figure 8: Digital representation (screen snapshot of Sound Forge window) of 1850 square waveform synthesized at a sampling frequency of 8000 Hz.

In addition to the above issue, there is also the problem of staircasing—the output of the digital-to-analog synthesizer jumps a little when it goes from one sample to the next, rather than continuing in a perfectly smooth trajectory. This may look harmless if you plot current versus time, but looks horrible when you plot the derivative. As a result inductive loads generate spurious voltage spikes between samples. For an experiment requiring a triangular waveform, the author first used a digital synthesizer capable of sampling rates of ~100 MHz (not kHz!). However the problems resulting from staircasing could not be sufficiently tamed, despite all attempts of filtering and smoothening, and in the end digital synthesis was abandoned in favor of an analog triangular waveform sources.

The advantages of digital audio are numerous—especially relating to its ease of storage and transmission. Its musical fidelity can also be excellent when its problems are controlled; the author uses a Theta® Generation series Digital-to-Analog Converter (http://www.thetadigital.com/) whose fidelity is quite satisfactory. However, one should be aware of the special problems that can arise, especially when digital sources are used for research. For some experiments the issues discussed above might not matter but for some they may change the outcome.

Readers wishing to replicate these experiments might find it easier to do Experiment 3 (the speaker-displacement one). The Aurum Cantus G2Si tweeters are inexpensive and easily available. The photograph shown in Fig. 6 explains the setup. All that is needed is a good analog square-wave generator (available from numerous instrument suppliers) and a high quality amplifier with good bandwidth and low output impedance (available at any high-end audio store). Some additional details about the equipment are given in the references Kunchur (2007) and Kunchur (2008).

Please also see the FAQ page for further information.

ACKNOWLEDGEMENTS

The author gratefully acknowledges G. Saracila and M. W. Rhoades for help with literature searching and other assistance, and acknowledges useful discussions and feedback from J. M. Knight, W. M. Hartmann, R. Meddis, F. G. Zeng, D. Oertel, E. W. Healy, R. A. Lutfi, R. D. Patterson, B. C. J. Moore, W. A. Yost, A. Botero, D. H. Wedell, K. Kubodera, R. White, and D. H. Arcos.

This work was partially supported by a grant from the University of South Carolina Office of Research and Health Sciences Research Funding Program.

REFERENCES

1. Eddins, D. A., Hall, J. W., and Grose, J. H. (1992). “Detection of temporal gaps as a function of frequency region and absolute bandwidth”, J. Acoust. Soc. Am. 91, 1069–1077.

2. Glasberg, B. R., and Moore, B. C. J. (1990). “Derivation of auditory filter shapes from notched-noise data”, Hearing Res. 47, 103–138.

3. Henning, B. G. (1974). “Detectability of interaural delay in high-frequency complex waveforms”, J. Acoust. Soc. Am. 55, 84–90.

4. Henning, G. B., and Gaskell, H. (1981). “Monaural phase sensitivity with Ronken’s paradigm”, J. Acoust. Soc. Am. 70, 1669–1673.

5. Krumbholz, K., Patterson, R. D., Nobbe, A., and Fastl, H. (2003). “Microsecond temporal resolution in monaural hearing without spectral cues?”, J. Acoust. Soc. Am. 113, 2790–2800.

6. Kunchur, M. N. (2007). “Audibility of temporal smearing and time misalignment of acoustic signals”, Electronic Journal Technical Acoustics, http://www.ejta.org, 2007, 17.
Preprint at: http://wind.physics.sc.edu/~kunchur/ARO2008/

7. Kunchur, M. N. (2008). “Temporal resolution of hearing probed by bandwidth restriction”, Acta Acustica united with Acustica 94, 594—603. **Preprint at: http://wind.physics.sc.edu/~kunchur/ARO2008/**

8. B. Leshowitz, “Measurement of the two-click threshold”, J. Acoust. Soc. Am. 49, 462–466 (1971).

9. van Maanen, H. R. E. (1993). “Temporal decay: a useful tool for the characterisation of resolution of audio systems?”, AES Preprint 3480 (C1-9), presented at the 94th convention of the Audio Engineering Society in Berlin.

10. J. O. Nordmark, “Binaural time discrimination”, J. Acoust. Soc. Am. 35, 870–880 (1976).

11. Patterson, R. D., and Datta, A. J. (1996). “The detection of iterated rippled niose (IRN) masked by IRN”, Br. J. Audiol., 30, 148.

12. Penner, M. J. (1977). “Detection of temporal gaps in noise as a measure of the decay of auditory sensation”, J. Acoust. Soc. Am. 61, 552–557.

13. Plomp, R. (1964). “Rate of decay of auditory sensation”, J. Acoust. Soc. Am. 36, 277–282.

14. Pollack, I. (1969). “Submicrosecond auditory jitter discrimination thresholds”, J. Acoust. Soc. Am. **45**, 1059–1059.

15. Pollack, I. (1971). “Spectral basis of auditory jitter discrimination”, J. Acoust. Soc. Am. **50**, 555.

16. Ronken, D. (1970). “Monaural detection of a phase difference between clicks”, J. Acoust. Soc. Am. 70, 1091–1099.

17. Stuart, J. R. (2004). “Coding for high-resolution audio systems”, J. Audio Eng. Soc., 52, 117–144.

18. Woszczyk, W (2003). “Physical and Perceptual Considerations for High-Resolution Audio”, Audio Engineering Society Convention Paper 5931 Presented at the 115th Convention 2003 October 10-13 New York, New York.

19. Yost, W. A., Patterson, R. D., and Sheft, S. (1996). “A time domain description for the pitch strength of iterated rippled noise”, J. Acoust. Soc. Am. 99, 1066–1078.